ARCHIVES
of
FOUNDRY ENGINEERING

ISSN (2299-2944)
Volume 2022
Issue 3/2022

11 – 18

2/3

10.24425/afe.2022.140231

Published quarterly as the organ of the Foundry Commission of the Polish Academy of Sciences

Elimination of Zinc from Aluminum During Remelting in an Vacuum Induction Furnace

A. Smalcerz [a, *], L. Blacha [a], B. Węcki [b], D.G. Desisa [c], J. Łabaj [a], M. Jodkowski [b]

[a] Faculty of Materials Engineering, Silesian University of Technology, Poland
[b] Department of Testing and Certification "ZETOM", Poland
[c] Department of Industrial, Informatics Silesian University of Technology, Joint Doctorate School, Poland
* Corresponding author. E-mail address: albert.smalcerz@polsl.pl

Received 18.03.2022; accepted in revised form 20.04.2022; available online 10.07.2022

Abstract

In this paper, the results of the study on aluminium evaporation from the Al-Zn alloys (4.2% weight) during remelting in a vacuum induction furnace (VIM) are presented. The evaporation of components of liquid metal alloys is complex due to its heterogeneous nature. Apart from chemical affinity, its speed is determined by the phenomena of mass transport, both in the liquid and gas phase. The experiments were performed at 10-1000 Pa for 953 K - 1103 K. A significant degree of zinc loss has been demonstrated during the analysed process. The relative values of zinc loss ranged from 4 to 92%. Lowering the pressure in the melting system from 1000 Pa to 10 Pa caused an increase in the value of density of the zinc evaporating stream from $3.82 \cdot 10^{-5}$ to 0.000564 $g \cdot cm^{-2} \cdot s^{-1}$ at 953 K and $3.32 \cdot 10^{-5}$ to 0.000421 $g \cdot cm^{-2} \cdot s^{-1}$ for 1103 K. Based on the results of the conducted experiments. it was found that evaporation of zinc was largely controlled by mass transfer in the gas phase and only for pressure 10 Pa this process was controlled by combination of both liquid and gas phase mass transfer.

Keywords: Mass transfer coefficient, Zinc evaporation, Vacuum induction furnace, Meniscus

1. Introduction

The evaporation of components of liquid metal alloys accompanies practically all technological operations related to their melting in various types of furnaces or high-temperature refining. It is of particular importance in operations under reduced pressure conditions. The evaporation process itself is complex due to its heterogeneous nature. Apart from chemical affinity, its speed is determined by the phenomena of mass transport, both in the liquid and gas phase. The chemical composition of the alloy, temperature and pressure changes as well as hydrodynamic conditions in the melting aggregate may significantly affect the rate of the evaporation process. Determining which of these factors has the most significant impact on the kinetics of the discussed process requires a lot of experimental research [1-2].

In this present analysis, authors investigated zinc elimination from molten aluminium and determined the main factor controlling their elimination. This experimental investigation was carried out in a vacuum induction furnace.

2. Metal evaporation criterion in vacuum

Due to the fact that the basic components of the tested alloy, i.e. aluminum and zinc, are characterized by a large difference in vapour pressures, it was assumed that the latter was eliminated from the liquid metal bath by its evaporation. The quantity determined by the thermodynamic point of view to ascertain the possibility of evaporation of the liquid component of a metallic

alloy is the so-called evaporation coefficient determined by the relationship [1]:

$$\Omega = \frac{\gamma_i \cdot p_i^o}{\gamma_j \cdot p_j^o} \quad (1)$$

Where p_i^o, p_j^o are equilibrium vapour pressure of the pure component *i* and *j* in Pa; γi, γ_j, are activity coefficient for component „i" and „j" in the liquid alloy.

When the $\Omega = 1$ condition is met, it is assumed that the alloy composition does not change during smelting. When $\Omega > 1$, we observe a loss in the alloy of component 'i' (due to evaporation) versus the 'j' component. When the $\Omega < 1$ condition is met, the situation is reversed.

To determine the values of the Ω coefficient the thermodynamic database HSC Chemistry ver. 6.1 was used [3]. In order to estimate the value of the Ω coefficient, the values of the equilibrium vapour pressure of the basic alloy components over molten metals were determined. For this thermodynamic data from the HSC Chemistry thermodynamic database was used. These values are summarized in Table 1.

Table 1.
Determined p_i^o values for, aluminum and zinc

	p_i^o, Pa						
Metal	953	978	1003	1028	1053	1078	1103
Aluminium	$7.7 \cdot 10^{-7}$	$2.1 \cdot 10^{-6}$	$5.5 \cdot 10^{-6}$	$1.4 \cdot 10^{-5}$	$3.3 \cdot 10^{-5}$	$7.6 \cdot 10^{-5}$	$1.7 \cdot 10^{-4}$
Zinc	6.1·103	$8.9 \cdot 10^{3}$	$1.3 \cdot 10^{4}$	$1.8 \cdot 10^{4}$	$2.5 \cdot 10^{4}$	$3.4 \cdot 10^{4}$	$2.5 \cdot 10^{4}$

The activity coefficients of Al and Zn in molten Al-Zn alloy were determined from the Krupkowski equations [4]:

$$\ln \gamma_{Al} = \left(\frac{1172.9}{T} - 0.4134\right) \cdot {X_{Zn}}^2 \quad (2)$$

$$\ln \gamma_{Zn} = \left(\frac{1172.9}{T} - 0.4134\right) \cdot \left[{X_{Zn}}^{1.8201} - \frac{1.8201}{1.8201-1} \cdot {X_{Zn}}^{1.8201-1} + \frac{1}{1.8201-1}\right] \quad (3)$$

Figure 1 shows changes in the Ω values versus temperature for the two basic alloy components. i.e. Al and Zn. For Zn and Al the $\Omega_{Zn/Al}$ values were over $1 \cdot 10^{-8}$. Thus the analysis showed that thermodynamically there is a potential for zinc evaporation from molten Al during its melting in the vacuum. This was confirmed by the results of investigations performed with the use of the vacuum induction furnace.

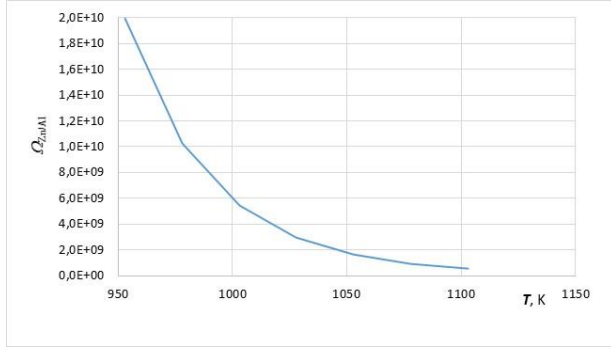

Fig. 1. Changes in the coefficient $\Omega_{Zn/Al}$ values versus temperature

3. Equipment and Experimental procedures

The research experiments were performed on a multi-component alloy; its composition is presented in Table 2.

Table 2.
Chemical composition of the Al-Zn alloy

Content of alloy components, wt. %									
Zn	Mg	Cu	Mn	Fe	Si	Cr	Ti	Zr	Al
4.2	1.2	<0.2	0.28	<0.4	<0.35	0.23	<0.05	0.014	residue

The melting system applied in the experiments was the Seco-Warwick VIM-20 vacuum induction melting furnace; its image is presented in Fig. 2.

The VIM 20-50 (PIT) furnace was equipped with:

- operator panel enabling control of operating parameters and control of the processes taking place in the furnace.
- system enabling the addition of alloy additives without disturbing the protective atmosphere.
- system enabling the ingot heating.
- sampling system.

At the beginning of each experiment an alloy sample (about 1000 g) was placed in an Isopress 1126-MG95I MgO crucible located inside the induction coil of the furnace. When the furnace chamber was closed a precisely specified vacuum was generated using diffusive and Roots pumps. After stabilising the chamber pressure the crucible was heated up to the set temperature. The temperature was measured with the use of a thermocouple sensor type B - PtRh30-PtRh6 and an optical pyrometer. During the experiment samples of the liquid alloy were taken and subjected to

chemical analysis. The analysis was carried out by atomic absorption spectrometry using the ASA Solar device.

Operating power, kW	8 -22
Vacuum, Pa	10 - 1000
Temperature, K	953 -1103

Fig. 2. The Seco-Warwick VIM-20 vacuum induction melting furnace

4. Research results and their discussion

4.1. Overall mass transfer coefficient

The data summarized in Table 4 shows that the determined losses of zinc mass from the tested alloy increased along with the decrease of the operating pressure of the furnace and it varied from 4 to 92%. Similarly, the increase of vacuum (1000-10 Pa) increased the value of the zinc evaporation flux from $3.82 \cdot 10^{-5}$ to $5.65 \cdot 10^{-4}$ g·cm^{-2}s^{-1} at 953 K and from $3.32 \cdot 10^{-5}$ to $4.21 \cdot 10^{-4}$ g·cm^{-2}s^{-1} at 1103 K. The decrease in the N_{Zn} flux density with the increase in temperature was caused by the increase in the size of the evaporation surface.

Table 4.
The data summarized

Alloy	P, kW	T, K	p, Pa	Final zinc concentration, % mas.	U_{Zn}, %	N_{Zn}, g·cm^{-2}s^{-1}
Al-Zn4.5Mg1	8	953	1000	4.01	4.52	$3.82 \cdot 10^{-05}$
Al-Zn4.5Mg1	8	953	500	3.62	13.81	$1.14 \cdot 10^{-04}$
Al-Zn4.5Mg1	8	953	100	3.01	28.33	$2.32 \cdot 10^{-04}$
Al-Zn4.5Mg1	8	953	10	1.25	70.24	$5.65 \cdot 10^{-04}$
Al-Zn4.5Mg1	12	1013	1000	3.66	12.86	$1.00 \cdot 10^{-04}$
Al-Zn4.5Mg1	12	1013	500	3.32	20.95	$1.64 \cdot 10^{-04}$
Al-Zn4.5Mg1	12	1013	100	2.77	34.05	$2.65 \cdot 10^{-04}$
Al-Zn4.5Mg1	12	1013	10	1.11	73.57	$5.64 \cdot 10^{-04}$
Al-Zn4.5Mg1	17	1073	1000	2.65	36.90	$2.45 \cdot 10^{-04}$
Al-Zn4.5Mg1	17	1073	500	2.37	43.57	$2.87 \cdot 10^{-04}$
Al-Zn4.5Mg1	17	1073	100	2.23	46.90	$3.08 \cdot 10^{-04}$
Al-Zn4.5Mg1	17	1073	10	0.89	78.81	$5.13 \cdot 10^{-04}$
Al-Zn4.5Mg1	22	1103	1000	1.16	72.38	$3.32 \cdot 10^{-04}$
Al-Zn4.5Mg1	22	1103	500	0.91	78.33	$3.57 \cdot 10^{-04}$
Al-Zn4.5Mg1	22	1103	100	0.54	87.14	$3.96 \cdot 10^{-04}$
Al-Zn4.5Mg1	22	1103	10	0.32	92.38	$4.21 \cdot 10^{-04}$

In order to determine the value of the overall mass transfer coefficient in the analysed evaporation process, it was assumed according to previous studies that it can be described by the first-order kinetic equation [2, 5]. Thus its rate can be described by the following relation:

$$\frac{dC_{Zn}}{dt} = k_{Zn} \cdot \frac{F}{V} \cdot C_{Zn} \tag{4}$$

This relationship in the integral form can be written as:

$$\int_0^t \frac{dC_{Zn}}{CZn} = k_{Zn} \cdot \frac{F}{V} \int_0^t dt \tag{5}$$

After integrating the relationships (5):

$$2.303 \log \frac{C_{Zn}^t}{C_{Zn}^0} = -k_{Zn} \frac{F}{V} (t - t_0) \tag{6}$$

Where C_{Zn}^0 and C_{Zn}^t are zinc concentration in the bath: initial and after time t in wt. %, F is the evaporation surface in m^2, V is the volume of liquid metal in m^3, $(t - t_0)$ is the duration of the process in s and k_{Zn} is the overall mass transfer coefficient in ms^{-1}.

Equation (6) shows that to determine the value of the k_{Zn} coefficient, it is necessary to know the volume of the melt and its surface. In the analysed experiments in the temperature range of 953-1103 K. The estimated value of the liquid metal volume was in the range from 419 to $425 \cdot 10^{-6}$ m^3. The values of liquid aluminium density in the analysed temperature range were determined based on the date contained in the publication [6-7]. They ranged from 2.35 to 2.38 g·cm^{-3}.

In the case of melting metal alloys in induction furnaces, we are dealing with an increase in the surface of the alloy through the formation of the so-called meniscus. For this reason, the method described in detail in [8] was used to determine the actual surface of the liquid Al-Zn alloy. This method allows you to estimate the size of the surface with the program Wolfram Mathematica. After taking a photo of the molten metal with a high-speed camera,

determination of the resulting geometry of the meniscus and determination of the functions of the curves describing the meniscus. Figure 3 shows an exemplary photo of a liquid alloy meniscus with marked points.

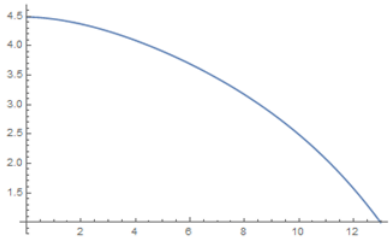

Fig. 3. Sample screenshot from the Wolfram Mathematica program of the meniscus of an aluminum alloy obtained in a crucible induction furnace

Table 5 summarizes the values of the meniscus surface area estimated for all experiments using.

Table 5.
The values of the area of meniscus formed for Al-Zn alloys

No.	P, kW	Alloy	F, cm^2	h_v, cm
1	8	Al	88.1	4.3
2	12	Al	92.4	5
3	17	Al	108.7	7
4	22	Al	155.0	10

Table 6.
The overall mass transfer coefficient k_{Zn} and coefficient β^l_{Zn} and k^e_{Zn}

P, kW	T, K	p, Pa	k_{Zn}, ms^{-1}	β^l_{Zn}	k^e_{Zn} ms^{-1}
8	953	1000	$3.814 \cdot 10^{-06}$	0.000548	$9.64 \cdot 10^{-05}$
8	953	500	$1.202 \cdot 10^{-05}$	0.000548	$9.64 \cdot 10^{-05}$
8	953	100	$2.696 \cdot 10^{-05}$	0.000548	$9.64 \cdot 10^{-05}$
8	953	10	$9.738 \cdot 10^{-05}$	0.000548	$9.64 \cdot 10^{-05}$
12	1013	1000	$1.050 \cdot 10^{-05}$	0.000541	$1.84 \cdot 10^{-04}$
12	1013	500	$1.583 \cdot 10^{-05}$	0.000541	$1.84 \cdot 10^{-04}$
12	1013	100	$3.199 \cdot 10^{-05}$	0.000541	$1.84 \cdot 10^{-04}$
12	1013	10	$9.961 \cdot 10^{-05}$	0.000541	$1.84 \cdot 10^{-04}$
17	1073	1000	$3.013 \cdot 10^{-05}$	0.000520	$4.33 \cdot 10^{-04}$
17	1073	500	$3.734 \cdot 10^{-05}$	0.000520	$4.33 \cdot 10^{-04}$
17	1073	100	$4.151 \cdot 10^{-05}$	0.000520	$4.33 \cdot 10^{-04}$
17	1073	10	$1.016 \cdot 10^{-04}$	0.000520	$4.33 \cdot 10^{-04}$
22	1103	1000	$5.908 \cdot 10^{-05}$	0.000475	$6.12 \cdot 10^{-04}$
22	1103	500	$6.982 \cdot 10^{-05}$	0.000475	$6.12 \cdot 10^{-04}$
22	1103	100	$9.375 \cdot 10^{-05}$	0.000475	$6.12 \cdot 10^{-04}$
22	1103	10	$1.185 \cdot 10^{-04}$	0.000475	$6.12 \cdot 10^{-04}$

The overall mass transport coefficient k_{Zn} were determined from equation 6 are shown in Table 6. Fig. 4 shows the graphical interpretation of the changes in the k_{Zn} coefficient as a function of the operating pressure of the induction furnace.

The data summarized in Table 6 shows that the reduction of the pressure in the furnace from 1000 to 10 Pa with a simultaneous increase in temperature from 953 K to 1103 K is accompanied by an increase in the value of the general mass transport coefficient k from $3.81 \cdot 10^{-6}$ - $1.18 \cdot 10^{-4}$ ms^{-1}. These values are in good agreement with the values given by other authors who investigated the process of evaporation of components of alloys melted in vacuum induction furnaces (Table 7).

Table 7.
Values of experimental mass transfer coefficients for the process of evaporation of liquid components of alloys melted in VIM technology

No.	The main component of the alloy	Metal removed	Temperature range, K	Pressure range, Pa	Mass transfer coefficient, ms^{-1}	References
1	Fe	Mn, Cu, Sn, Cr	1873	0.1-1333	$0.96\text{-}8.4\cdot10^{-5}$	[9-17]
2	Ti	Al, Mn	1973-2023	5-1000	$0.97\text{-}3.74\cdot10^{-5}$	[2, 17-19]
3	Cu	Pb, Sb, As, Bi	1373-1740	0.1-1333	$1.0\text{-}30\cdot10^{-5}$	[2, 20-22]
4	Al	Zn	953-1103	8-1000	$3.81\cdot10^{-6}\text{-}1.18\cdot10^{-4}$	Present work

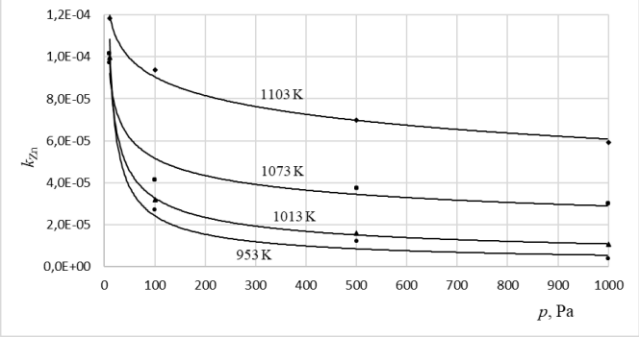

Fig. 4. Variation of overall mass transfer coefficient k_{Zn} vs. pressure

4.2. Liquid phase mass transfer

Transfer of alloy components through molten metal to the melt surface can be represented by the Machlin model [23]. According to this model, determining the value of the transport coefficient of zinc β^l is recommended with equation:

$$\beta^l = \left(\frac{8\, D_{Zn}\, \vartheta_m}{\pi\, r_m}\right)^{0.5} \tag{7}$$

Where v_m is mean surface velocity, r_m is the radius of the surface of the liquid metal (most often taken as the inner radius of the crucible and DAs is the diffusivity of zinc in molten aluminium.

Machlin assumed for induction furnaces with a capacity of up to 1Mg that the value of speed v_m was constant and was 0.1 ms^{-1}. However, in later studies, it was shown that this speed depends on factors such as the frequency of the current, the geometry of the crucible, or the position of the crucible in the furnace relative to the inductor
[24-26].

The previously discussed works [18, 27-28] also presented a simulation model that allows determining the value of the mean surface velocity of copper during its melting for the same aggregate that was used in the analysed studies on zinc removal. This model consisted of two successive elements. i.e. the analysis of the electromagnetic field generated in the liquid metal and the analysis of the velocity field occurring in the liquid metal.

Table 3 presents the values of the β^l coefficient determined from equation (5). The values were within range of the analysed temperatures; from 5.48 to $4.75\cdot10^{-4}$ ms^{-1}. The value of zinc diffusion coefficients in liquid aluminium was estimated on the basis of data contained in the paper [29]. Estimated values of the $D_{Zn\text{-}Al}$ coefficient were $5.12\text{-}5.25\cdot10^{-4}$ cm^2s^{-1} in the temperature range of 953-1103 K.

4.3. Transfer from surface to gas phase

When analysing the rate of zinc evaporation from the surface of the liquid alloy, it was assumed that the maximum value of the evaporation mass transfer coefficient k^e_{Zn} is described by the relationship [5]:

$$k^e_{Zn} = \frac{\alpha\cdot\psi}{(2\pi RTM_{Zn})^{0.5}} \tag{8}$$

Where M_{Zn} is molar mass of Zn, R is gas constant, T is temperature, α is relative volatility coefficient and ψ is multiplier.

$$\psi = \frac{\gamma_{Zn}\ M_{Al}P^0_{Zn}}{\rho_{Al}} \tag{9}$$

Where γ_{Zn} is activity coefficient of Zn, M_{Al} is molar mass of Al, P^0_{Zn} is equilibrium Zinc vapour pressure and ρ_{Al} is density of molten aluminium.

Fig. 5 shows the change of the k^e_{Zn} coefficient in the temperature range 953-1113 K determined from the equation (8).

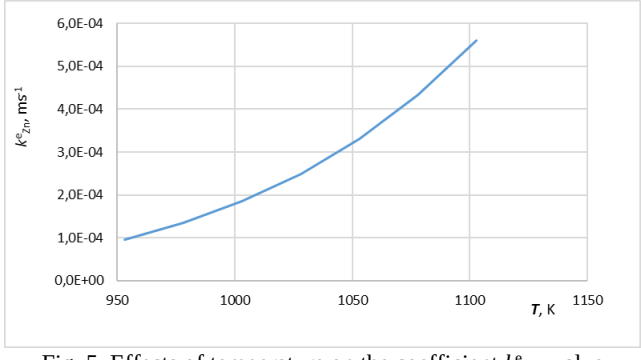

Fig. 5. Effects of temperature on the coefficient k^e_{Zn} value

Fig. 7 shows the estimated values participation of summary of resistance associated with the evaporation reaction (R^e) and resistance mass transfer in the liquid phase ($R^{\beta l}$) in the total resistance of the zinc evaporation process. The following equations were used for this:

$$R^{e} = \frac{\left(\frac{1}{k^{e}_{Zn}}\right)}{\left(\frac{1}{k_{Zn}}\right)} \cdot 100\,\% \tag{10}$$

$$R^{\beta l} = \frac{\left(\frac{1}{\beta^{l}_{Zn}}\right)}{\left(\frac{1}{k_{Zn}}\right)} \cdot 100\,\% \tag{11}$$

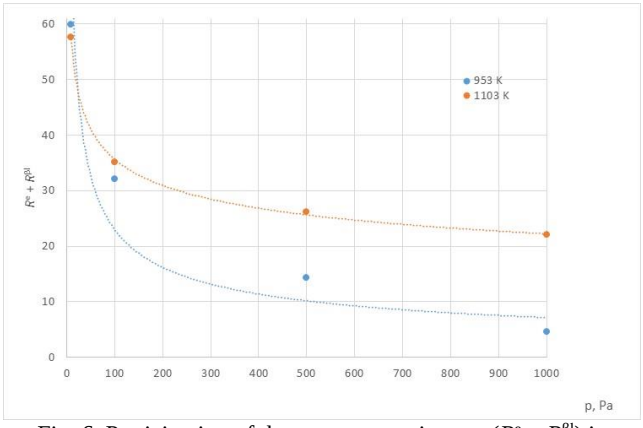

Fig. 6. Participation of the summary resistance ($R^{e} + R^{\beta l}$) in overall resistance of Zn evaporation process

With pressures in the furnace from 100 to 1000 Pa and the analysed temperature range, the process of zinc evaporation from liquid aluminium is determined by mass transfer in the gas phase. The total resistance related to mass transfer in the liquid phase ($R^{\beta l}$) and the reaction on the surface of the liquid metal (R^{e}) accounts for 30 to 35% of the total process resistance. Lowering the pressure to 10 Pa increases the value of the total resistance ($R^{\beta l} + R^{e}$) to 65% (Fig. 6).

The data presented in Fig. 7 shows that for the ranges of temperatures and pressures used in the experiments, the share of mass transport resistance in molten metals in the total process resistance is in the range of 0.7-45%. As the pressure decreases, this resistance increases. In the case of resistance related to the evaporation reaction in itself, its share in the total process resistance was in the range of 3.8-31% (Fig. 8).

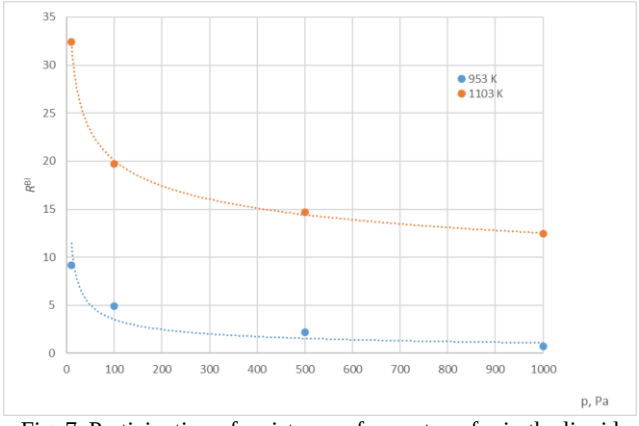

Fig. 7. Participation of resistance of mass transfer in the liquid phase ($R^{\beta l}$) in overall resistance of evaporation process

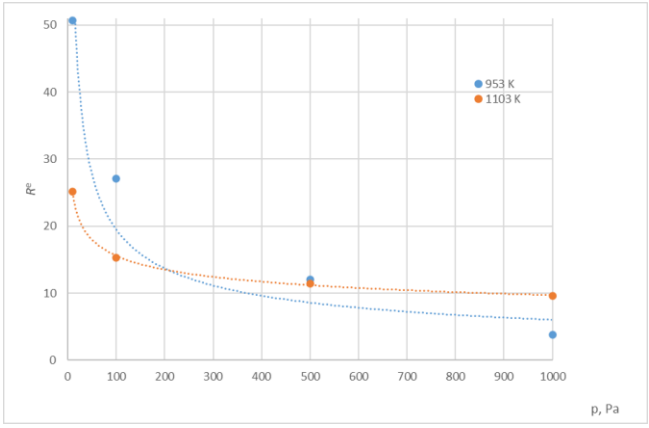

Fig. 8. Participation of resistance of the reaction on the surface of the liquid metal (R^{e}) in overall resistance of evaporation process

4.4. Mass transfer in gas phase

None of the known hydrodynamic models used to describe mass transport in the gas phase allow for an accurate estimation of the value of the mass transport coefficient β^{g} Zn for the measuring systems used in research. For this reason, the *OPR* (Over Pressure Ratio) parameter was used to determine the role of mass transfer within the gas phase in the analysed zinc evaporation process as proposed in [30]. The *OPR* parameter is defined as the ratio of the total initial pressure of the bath components above the alloy to the pressure in furnace chamber.

$$OPR = \frac{\sum_{i=1}^{n} p_i}{p_{ch}} \tag{12}$$

It is assumed that transport in the gas phase does not determine the rate of the analysed metal evaporation process under reduced pressure conditions when the following condition is met:

$$OPR > 1 \tag{13}$$

By analysing the obtained results, the *OPR* coefficient was estimated for the temperature range in which the experiments were conducted. It was adapted to take into account the composition of the alloy the vapour pressure of not only zinc but also aluminium and magnesium. The results of these calculations are presented graphically in Fig. 9.

The data presented in Fig. 9 shows that the relation (13) is fulfilled only for the pressure of 10 Pa. This confirms the previous observations that for pressures of 100-1000 Pa. The analysed process is controlled by mass transport in the gas phase.

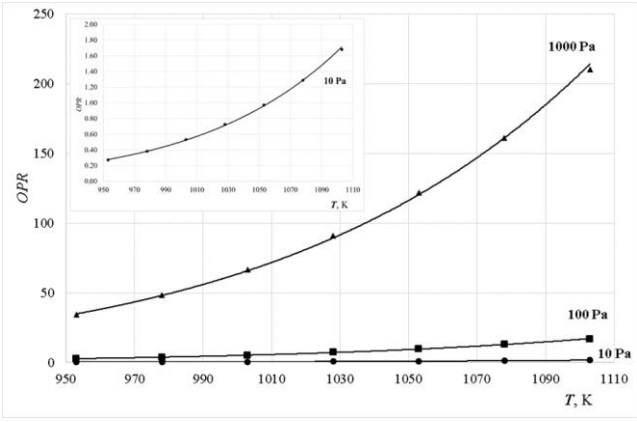

Fig. 9. Effects of temperature on the coefficient k^{e}_{Zn} value

5. Summary

In the paper results of the study of zinc evaporation from the Al-Zn alloy during melting in a vacuum induction furnace (VIM) are presented. The alloy analysed contained 4.2 wt. % of zinc. The tests were carried out in the Seco-Warwick VIM-20 vacuum induction furnace. The results obtained were used to determine an experimental overall mass transfer coefficient k_{Zn} namely the basic kinetic parameter characterizing analysing process. At the same time, mass transfer coefficient in the liquid phase (β^{l}) and coefficient k_e were determined.

Based on the results of the conducted experiments it was found that:

- Change of the chamber pressure from 1333 to 10 Pa with a simultaneous increase in temperature from 953 K to 1103 K accompanied by a decrease in the zinc content in the alloy from 4 to 92% compared to the initial concentration.
- At the same time the value of the general mass transport coefficient k grows from $3.81 \cdot 10^{-6}$ - $1.18 \cdot 10^{-4}$ ms^{-1}.
- Elimination of zinc was largely controlled by mass transfer in gas phase.
- Only for pressure 10 Pa the rate of Zn evaporation controlled by the combination of both liquid and gas phase mass transfer in the all pressure range. The participation of resistance related to mass transport in the liquid phase in the total process resistance does not exceed 32% and the resistance related to the act of evaporation itself does not exceed 31%.
- The increase in the value of the furnace operating power from 8 to 22 kW increases the surface area of the liquid aluminium alloy above 50%.

Acknowledgement

This work was supported by the Silesian University of Technology, grant No. 11/020/BK_21/0080, and grant No. 11/040/BK_21/0023. The authors declare they have no conflict of interest.

References

[1] Guo, J., Liu, Y. & Su, Y. (2002). Evaporation of multi-components in Ti-25Al-25Nb melt during induction skull melting process. *Transaction of Nonferrous Metals Society of China*. 12(4), 587-591.
[2] Blacha, L., Mizera, J. & Folega, P. (2013). The effects of mass transfer in the liquid phase on the rate of aluminium evaporation from the Ti-6Al-7Nb alloy. *Metalurgija*, 53(1), 51-54.
[3] HSC Chemistry ver. 6.1. Outocumpu Research Oy. Pori.
[4] Plewa, J. (1987). *Examples of calculations from the theory of metallurgical processes*. Gliwice: Wydawnictwo Politechniki Śląskiej. (in Polish).
[5] Ozberk, E. & Guthrie, R. (1986). A kinetic model for the vacuum refining of inductively stirred copper melts. *Metallurgical Transactions B.* 17, 87-103.
[6] Nash, P.M. & Steinemann, S.G. (2006). Density and thermal expansion of molten manganese. Iron. Nickel. Copper. Aluminium and Tin by Means of the Gamma-Ray Attenuation Technique. *Physics and Chemistry of Liquids, An International Journal*. 29(1), 43-58.
[7] Assael, M., Kakosimos, K. & Banish, R. (2006). Reference data for the density and viscosity of liquid aluminum and liquid iron. *Journal of Physical and Chemical Reference Data.* 35(1), 285-301.
[8] Smalcerz, A., Węcki B. & Blacha L. (2021) Influence of the power of various types of induction furnaces on the shape of the metal bath surface. *Advances in Science and Technology Research Journal*. 15(3), 34-42. DOI:10.12913/22998624/138245
[9] Homma, M., Ohno, R., & Ishida, T. (1996). Evaporation of manganese. copper. and tin from molten iron under, vacuum. *Science Reports of the Research Institutes, Tohuku University. Series A – Physics. chemistry and metallurgy*. 18, 356-365.
[10] Ohno, R. & Ishida, T. (1967). Solution rate of solid iron in liquid copper, *ISIJ International*. 31(10), 1164-1169.
[11] Chen, X. & Ito, N. (1995). Evaporation rate of copper in high carbon iron melt under reduced pressure. *Tetsu-to-Hagane*. 81(10), 959-964.
[12] Savov, L. & Janke, D. (2000). Evaporation of cu and sn from induction-stirred iron-based melts treated at reduced pressure. *ISIJ International*. 40(2), 95-104.
[13] Łabaj, J. (2012). Kinetics of cooper evaporation from the Fe-Cu Alloys under Reduced Pressure. *Archives of Metallurgy and Materials.* 57(1), 165-172.
[14] Maruyama, T., Katayama, H., Momono, T., Tayu, Y, & Takenouchi, T. (1998). Evaporation rate of copper from molten iron by urea spraying under reduced pressure. *Tetsu-to-Hagane*. 84(4), 243-248.
[15] Ono-Nakazato, H. & Taguchi, K. (2003). Effect of silicon and carbon on the evaporation rate of copper in molten iron. *ISIJ International*. 43(11), 1691-169.
[16] Bellot, J.P., Duval, H., Ritchie, M., Mitchell, A. & Ablitzer, D. (2001). Evaporation of Fe and Cr from induction-stirred austenitic stainless steel-influence of the inert gas pressure, *ISIJ International*. 41(7), 696-705.

[17] Siwiec, G. (2013). The kinetics of aluminium evaporation from the Ti-6Al-4V alloy. *Archives of Metallurgy and Materials*. 58(4), 1155-1160.
[18] Blacha, L. Golak, S. Jakovics, S. & Tucs A. (2014) Kinetic analysis of aluminum evaporation from Ti-6Al-7Nb. *Archives of Metallurgy and Materials*. 59, 275-279. DOI: 0.2478/amm-2014-0045.
[19] Blacha, L., Burdzik, R. Smalcerz, A. & Matuła, T. (2013). Effects of pressure on the kinetics of manganese evaporation from the OT4 alloy. *Archives of Metallurgy and Materials*. 58(1), 197-201.
[20] Harris, R. (1984). Vacuum refining copper melts to remove bismuth, arsenic and antimony. *Metallurgical Transaction B.* 15, 251-257.
[21] Harris, R., McClincy, R.J. & Riebling, E.F. (1987). Bismuth, arsenic and antimony removal from anode copper via vacuum distillation. *Canadian Metallurgical Quarterly*. 26(1), 1-4.
[22] Ozberk, B., Guthire, R.I.L. (1987). Vacuum melting of copper evaporation – evaporation of impurities. Proc. 6th Int. Vacuum Metallurgy Conf. American Vacuum Society. San Diego. 248-267.
[23] Machlin, E.S. (1961). Kinetics of vacuum induction refining – theory. the american institute of mining. Metallurgical. and Petroleum Engineers.
[24] Tarapore, E.D. & Evans, J. (1976). Fluid velocities in induction melting furnaces: Part I. Theory and laboratory experiments. *Metallurgical Transaction B*. 7, 343-351.
[25] Tarapore, E.D., Evans, J. & Langfeld**,** J. (1977). Fluid velocities in induction melting furnaces: Part II. large scale measurements and predictions. *Metallurgical Transaction B*. 8, 179-184.
[26] Szekely, J., Chang, W. & Johnson, W. (1977). Experimental measurement and prediction of melt surface velocities in a 30.000 lb inductively stirred melt. *Metallurgical Transaction B*. 8, 514-517.
[27] Przyłucki, R. Golak, S. Oleksiak, B. & Blacha L. (2012). Influence of an induction furnace's electric parameters on mass transfer velocity In the liquid phase. *Metalurgija*. 1, 67-70.
[28] Blacha, L. Przylucki, R. Golak, S. & Oleksiak B. (2011). Influence of the geometry of the arrangement inductor - crucible to the velocity of the transport of mass in the liquid metallic phase mixed inductive. *Archives of Civil and Mechanical Engineering*. 11, 171-179 DOI: 10.1016/S1644-9665(12)60181-2
[29] Du, Y., Chang, Y., Huang, B., Gong, W. & Jin, Z. (2003). Diffusion coefficients of some solutes in fcc and liquid Al: critical evaluation and correlation. *Materials Science and Engineering: A*. 363(1-2), 140-151.
[30] Harris, R. & Davenport, W.G. (1982). Vacuum distillation of liquid metals: Part I. Theory and experimental study. *Metallurgical Transactions B.* 13, 581-588.